The THO/TREX Complex Active in miRNA Biogenesis Negatively Regulates Root-Associated Acid Phosphatase Activity Induced by Phosphate Starvation[1][OPEN]

Sibo Tao[2], Ye Zhang[2], Xiaoyue Wang, Le Xu, Xiaofeng Fang, Zhi John Lu, and Dong Liu*

MOE Key Laboratory of Bioinformatics, Center for Plant Biology, School of Life Sciences, Tsinghua University, Beijing 100084, China

ORCID ID: 0000-0002-4679-3515 (D.L.).

Induction and secretion of acid phosphatases (APases) is an adaptive response that plants use to cope with P (Pi) deficiency in their environment. The molecular mechanism that regulates this response, however, is poorly understood. In this work, we identified an Arabidopsis (*Arabidopsis thaliana*) mutant, *hps8*, which exhibits enhanced APase activity on its root surface (also called root-associated APase activity). Our molecular and genetic analyses indicate that this altered Pi response results from a mutation in the *AtTHO1* gene that encodes a subunit of the THO/TREX protein complex. The mutation in another subunit of this complex, AtTHO3, also enhances root-associated APase activity under Pi starvation. In Arabidopsis, the THO/TREX complex functions in mRNA export and miRNA biogenesis. When treated with Ag^+, an inhibitor of ethylene perception, the enhanced root-associated APase activity in *hps8* is largely reversed. *hpr1-5* is another mutant allele of *AtTHO1* and shows similar phenotypes as *hps8*. *ein2* is completely insensitive to ethylene. In the *hpr1-5ein2* double mutant, the enhanced root-associated APase activity is also greatly suppressed. These results indicate that the THO/TREX complex in Arabidopsis negatively regulates root-associated APase activity induced by Pi starvation by inhibiting ethylene signaling. In addition, we found that the miRNA399-PHO2 pathway is also involved in the regulation of root-associated APase activity induced by Pi starvation. These results provide insight into the molecular mechanism underlying the adaptive response of plants to Pi starvation.

Although phosphorus (P) is abundant in most soils, the amount of inorganic P (Pi), the major form of P that plants assimilate, is limited (Raghothama, 2000). This is because the majority of P in these soils exists as organophosphates or is fixed with metals, which makes Pi highly immobile. To cope with Pi deficiency, plants activate a set of adaptive responses to reprioritize internal Pi use and to enhance external Pi acquisition (Yuan and Liu, 2008). Induction and secretion of acid phosphatases (APase) is a universal response of plants to Pi starvation and is regarded as an important way by which plants scavenge Pi from external organophosphates (Tran et al., 2010a). Indeed, knockout or overexpression of some APase genes significantly affects plant utilization of external organic P (Hurley et al., 2010; Robinson et al., 2012; Wang et al., 2009, 2011, 2014).

Pi starvation-induced (PSI) APases have been biochemically characterized in several plant species (Tran et al., 2010a) and have been extensively studied in Arabidopsis (*Arabidopsis thaliana*; del Pozo et al., 1999; Zhu et al., 2005; Veljanovski et al., 2006; Tran et al., 2010b; Wang et al., 2011, 2014; Robinson et al., 2012; Del Vecchio et al., 2014). Although there are 44 annotated APase genes in Arabidopsis (Li et al., 2002), three APases (AtPAP10, AtPAP12, and AtPAP26) of the Arabidopsis purple acid phosphatase (AtPAP) family together account for most of the PSI APase activity on the root surface (also called root-associated APase activity) (Wang et al., 2011, 2014; Robinson et al., 2012). Among these three APases, AtPAP12 and AtPAP26 are also major intracellular APases (Veljanovski et al., 2006; Tran et al., 2010b; Robinson et al., 2012; Wang et al., 2014). In contrast, AtPAP10 is mainly a secreted APase and is predominantly associated with the root surface after secretion (Wang et al., 2011). The triple knockout *atpap10/12/26* mutant retains only about 20% of the root-associated APase activity of the wild type (Wang et al., 2014). Suc and ethylene have been identified as two positive regulators of PSI root-associated APase activity (Lei et al., 2011a, 2011b; Yu et al., 2012; Wang et al., 2012). Suc seems to act as a systemic signal that moves from shoots to roots to regulate transcription of *AtPAP10* mRNA while ethylene serves as a local signal that mainly affects the secretion of AtPAP10 proteins or AtPAP10 enzymatic activity on the root surface (Zhang

---

et al., 2014). In bacteria and yeast, the signaling pathway involved in this Pi scavenging system, the so-called PHO regulon, has been well established (Lenburg and O'Shea, 1996; Wanner, 1996). Although a plant PHO regulon had also been proposed (Goldstein et al., 1988), a different and more complex regulatory network is believed to control PSI root-associated APase activity in higher plants. Ethylene, for example, plays an important role in the regulation of root-associated APase in Arabidopsis but is not found in bacteria and yeast (Lei et al., 2011b; Wang et al., 2012; Yu et al., 2012).

MicroRNAs (miRNAs), which have 21 to 24 nucleotides, are a class of small regulatory RNAs. Biogenesis of miRNAs requires the activity of RNA polymerase II, which produces complementary, long, dsRNA precursors; these precursors are cleaved by DICER-LIKE (DCL) proteins and processed into mature miRNAs (Margis et al., 2006). The cleaved double-stranded miRNAs then become associated with ARGONAUTE proteins to inhibit the expression of their target genes through either degradation of target mRNAs or blockage of protein translation (Mallory and Vaucheret, 2006). These small RNAs participate in a variety of biological processes, including plant responses to external stresses. Several miRNAs have been determined to be involved in plant responses to nutrient deficiency. The level of miRNA395, for example, is up-regulated during plant responses to sulfur deprivation (Liang et al., 2010). This miRNA targets two families of genes, ATP sulfurylases and sulfate transporter 2;1, both of which are involved in sulfate metabolism. miRNA827 targets the mRNA of *NITROGEN LIMITATION ADAPTATION*, which encodes a ubiquitin E3 ligase (Kant et al., 2011). Interestingly, miRNA827 transcription is specifically induced by Pi deprivation. Subsequent research demonstrated that miRNA827 modulates Pi transporter activity by affecting the *NITROGEN LIMITATION ADAPTATION*-mediated degradation of Pi transporters (Lin et al., 2013). The miRNA whose function in response to nutrient deficiency has been best characterized is miRNA399 (Kuo and Chiou, 2011). miRNA399 is rapidly induced by Pi deficiency. It targets *PHO2* mRNA, which encodes a ubiquitin E2 conjugase. When plants are exposed to Pi deficiency, increased miRNA399 enhances plant Pi uptake capacity by reducing the level of PHO2 proteins, thus stabilizing the Pi transporters on the root surface (Huang et al., 2013). Under Pi sufficiency, overexpression of *miRNA399* or knockout of *PHO2* leads to an over-accumulation of Pi in shoots. Although the role of the miRNA399-PHO2 pathway in Pi signaling has been well established, to date, its specific function in the control of PSI root-associated APase activity remains unknown.

In this work, we identified an Arabidopsis mutant, *hps8*, with enhanced PSI root-associated APase activity. The mutant phenotypes are caused by a mutation in *AtTHO1*, which encodes a component of the THO/TREX complex; this complex is involved in the export of mRNAs from the nucleus and in the biogenesis of

miRNAs and siRNAs in Arabidopsis (Furumizu et al., 2010; Jauvion et al., 2010; Yelina et al., 2010). Our research indicates that the THO/TREX complex negatively regulates PSI root-associated APase activity by suppressing ethylene signaling. The analysis of miRNA expression profiles in *hps8* also led us to discover that the miRNA399-PHO2 module is another important regulator of PSI root-associated APase activity.

RESULTS

Characterization of the Arabidopsis Mutant *hps8*

To identify novel molecular components involved in the control of PSI root-associated APase activity, we performed a genetic screen for Arabidopsis mutants with altered APase activity on the root surface. Arabidopsis seeds harvested from EMS-mutagenized plants were sown on Pi-deficient (P⁻) medium. Eight days after seed germination, an agar solution containing an APase substrate, 5-bromo-4-chloro-3-indolyl-P (BCIP), was overlaid on the roots of the seedlings. The cleavage of the substrate by the APases produces a blue precipitate. On the root surface of wild-type seedlings grown on Pi-sufficient (P⁺) medium, no blue staining was detected (Fig. 1A). In contrast, blue staining occurred on the root surface of wild-type seedlings grown on P⁻ medium. Using this method, we identified an Arabidopsis mutant that showed enhanced BCIP staining on its root surface compared to that of the wild type under Pi deficiency (Fig. 1A). The mutant was designated *hypersensitive to Pi starvation8* (*hps8*). *hps8* also displayed light-blue staining when grown on P⁺ medium (Fig. 1A). The enhanced root-associated APase activity in *hps8* was confirmed by quantitative analysis using BCIP as a substrate (Fig. 1B). To understand the cause of the enhanced root-associated APase activity in *hps8*, we analyzed the transcription of three major APase genes: *AtPAP10*, *AtPAP12*, and *AtPAP26*. The results showed that the transcription of these three APase genes in *hps8* did not significantly differ from that of the wild type under P⁺ condition; under P⁻ condition, however, the transcription of *AtPAP10* and *AtPAP12* was reduced 30% and 50%, respectively, in *hps8*, whereas transcription of *AtPAP26* was unchanged (Supplemental Fig. S1). Interestingly, the total root intracellular APase activity of the wild type did not significantly differ from that of *hps8* (Fig. 1C). These results suggested that the enhanced root-associated APase activity in *hps8* might be due to altered posttranslational processes, such as increased secretion of APase proteins or increased APase enzymatic activity on the root surface.

Pi deficiency reduces primary root growth and enhances the production of lateral roots and root hairs (Williamson et al., 2001; Linkohr et al., 2002). The growth of the primary root of the wild type and *hps8* was similar on agar plates regardless of Pi conditions (Fig. 2A). The length of root cells and the size of the root apical meristem were also similar in the wild type and *hps8* (Supplemental Fig. S2). On P⁺ medium, however,
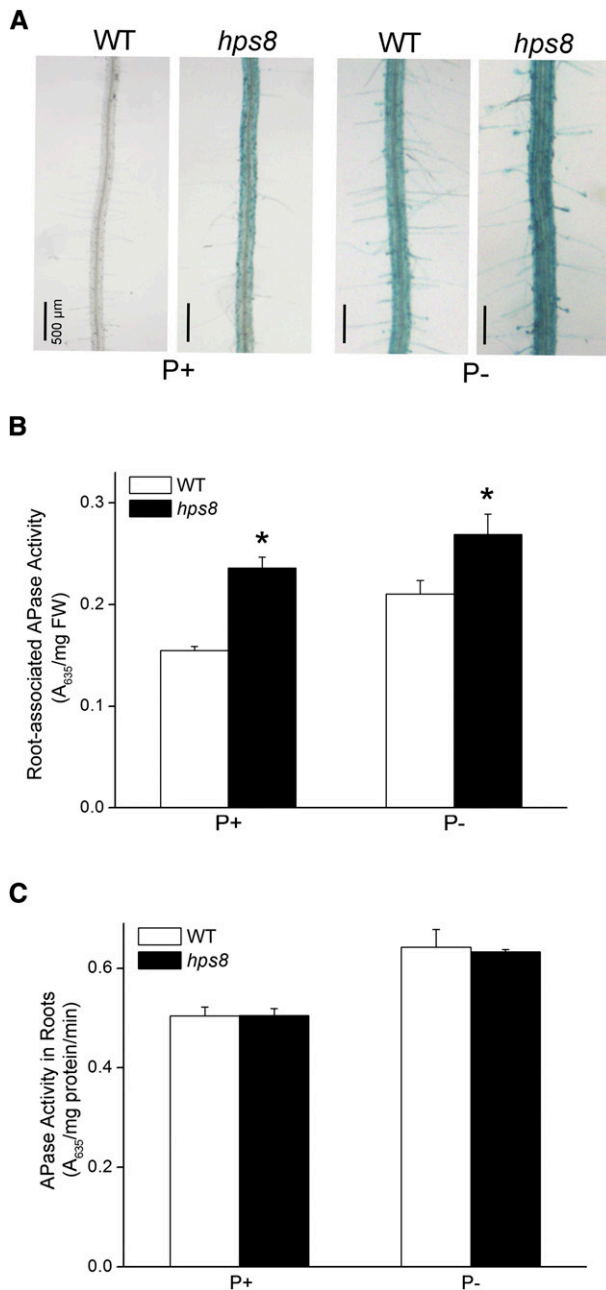
Figure 1. Analysis of Pi starvation-induced root APase activity in 8-d-old Arabidopsis seedlings of the wild type and *hps8*. A, Histochemical staining of APase activity on the root surface of the seedlings using BCIP as a substrate. B, Root surface-associated APase activity as determined with BCIP as the substrate. C, Root intracellular APase activity as determined with BCIP as the substrate. Values in B and C represent means with sᴇ of three replicates. Asterisks indicate significant difference ($P <$ 0.05) from the wild type according to Student's *t* test.

the *hps8* seedlings had fewer and shorter lateral roots than the wild type. This difference in lateral roots was not evident when plants were grown on P⁻ medium. *hps8* also produced more and longer root hairs than the wild type under both P⁺ and P⁻ conditions (Fig. 2B).

When grown in soil, *hps8* plants were smaller than the wild type and had serrated leaves (Fig. 3D).

The contents of total P and cellular Pi in shoots and roots did not significantly differ between *hps8* and the wild type (Supplemental Fig. S3).

HPS8 Encodes a Subunit of the THO/TREX Complex

Analyses of F1 and F2 progeny derived from a cross between *hp8* and a wild-type plant indicated that the mutant phenotypes of dark-blue BCIP-staining, enhanced root hair production, and small plant size were closely linked and could be attributed to a single recessive mutation. A map-based cloning approach was used to identify the molecular lesion in *hps8*. Using a set of molecular markers (Supplemental Table S1), we mapped the *hps8* mutation to a 74-kb region on chromosome 5 (Supplemental Fig. S4). After all 20 annotated genes in this interval were sequenced, a point mutation was found in the first exon of the *AtTHO1* gene (At5G09860; (Fig. 3A). This mutation caused a single nucleotide change of C to T, resulting in a conversion of an Arg to a stop codon. The introduced premature stop codon was located at the position of the 10th amino acid, which terminated the translation of almost the entire AtTHO1 protein. Hereafter, we refer to *HPS8* as *AtTHO1*.
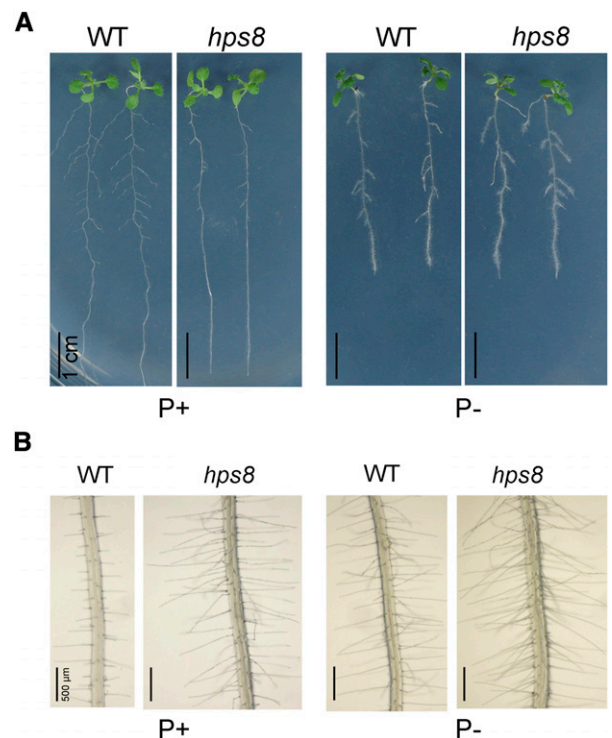

Figure 2. Root morphological phenotypes of 8-d-old Arabidopsis seedlings of the wild type and *hps8* grown under Pi sufficiency (P⁺) and deficiency (P⁻) conditions. A, The whole seedlings showing root growth characteristics. B, Patterns of root hair formation.
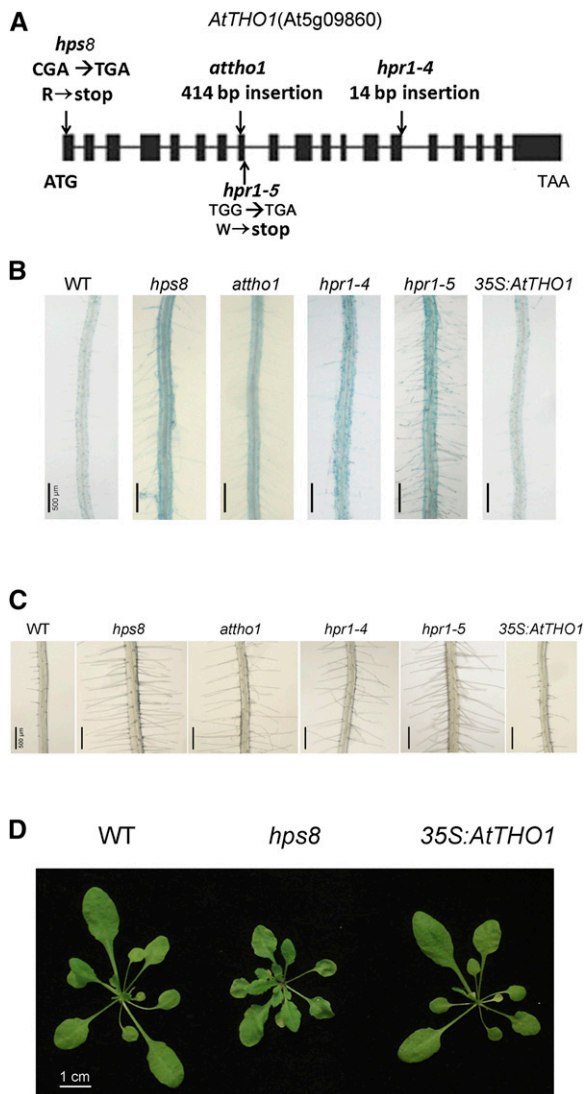
Figure 3. Molecular and genetic analyses of *hps8*. A, A diagram showing the structure of the *AtTHO1* gene and the positions of the point mutation in the *hps8* and *hpr1-5* mutants and the insertions in the *attho1* and *hpr1-4* mutants. The black box and the horizontal line represent the exons and introns, respectively. The positions of start (ATG) and stop (TGA) codons are shown. B, Histochemical staining of APase activity on the root surface of 8-d-old seedlings of the wild type, *hps8*, *attho1*, *hpr1-4*, *hpr1-5*, and *35S:AtTHO1* grown on P⁺ medium. C, Root hair patterns of the seedlings corresponding to those shown in B. D, Morphologies of 3-week-old plants of the wild type, *hps8*, and *35S:AtTHO1* grown in soil.

AtTHO1 shares homology with HPR1, a subunit of the THO/TREX protein complex that is conserved in yeast, animals, and humans. This protein complex functions in transcription elongation and mRNA export from the nucleus (Strässer et al., 2002; Rehwinkel et al., 2004; Katahira, 2012). The THO/TREX complex consists of seven subunits, and the counterparts of all seven subunits have been found in *Arabidopsis*. Five independently identified mutant alleles of *AtTHO1* (*attho1*,

hpr1-1, *emu*, *hpr1-4*, and *hpr1-5*) were previously reported (Yelina et al., 2010; Jauvion et al., 2010; Furumizu et al., 2010; Pan et al., 2012; Xu et al., 2015). Like *hps8*, the mutants *attho1*, *hpr1-4*, and *hpr1-5* exhibited enhanced BCIP staining on their root surfaces and produced more root hairs than the wild type under both P⁺ and P⁻ conditions (Fig. 3, B and C; data not shown). These results suggested that *hps8* was another mutant allele of *AtTHO1*.

To further confirm that the mutant phenotypes of *hps8* were caused by the mutation in the *AtTHO1* gene, we introduced the wild-type genomic sequence of *AtTHO1* into *hps8* plants under the control of the Cauliflower Mosaic Virus 35S (*CaMV 35S*) promoter. The expression of the wild-type *AtTHO1* gene fully restored the mutant phenotypes of *hps8* with respect to BCIP staining, root hair production, and plant size (Fig. 3, B–D). Taken together, our results demonstrated that the mutation in the *AtTHO1* gene was responsible for all of the *hps8* phenotypes.

AtTHO1 Is Ubiquitously Expressed and Is Localized in the Nucleus

To analyze the expression patterns of *AtTHO1*, we performed qPCR using RNAs extracted from different tissues. The results showed that *AtTHO1* expression was higher in flowers and siliques than in roots, stems, and leaves and was similar among the latter three organs (Fig. 4A). The expression of *AtTHO1* mRNA was slightly increased by Pi starvation in roots but not in shoots (Fig. 4B).

To determine the subcellular localization of AtTHO1 protein, we fused a GFP gene to the N terminus of *AtTHO1* and transformed this fusion gene into wild-type plants under the control of the *CaMV 35S* promoter. In the root cells of the transgenic plants, a strong green fluorescence signal was observed in the nucleus (Fig. 4C), indicating that AtTHO1 is a nuclear-localized protein.

The THO/TREX Complex Negatively Regulates PSI Root-Associated APase Activity

In Arabidopsis, four of the seven subunits of the THO/TREX complex (AtTHO1, AtTHO2, AtTHO3, and AtTHO6) are encoded by a single gene. The homozygote mutant of *AtTHO2* (At1g24706) is embryolethal (Furumizu et al., 2010). To investigate whether the other two subunits of THO/TREX complex are involved in the regulation of PSI root-associated APase activity, we analyzed the effects of mutations of *AtTHO3* (At5g56130) and *AtTHO6* (At2g19430) genes. *attho3* behaved like *hps8* in exhibiting enhanced BCIP staining and overproduction of root hairs, but *attho6* looked like the wild type (Fig. 5). These results indicated that the Arabidopsis THO/TREX complex negatively regulates PSI root-associated APase activity and that different components of this complex contribute differently to plant responses to Pi starvation.
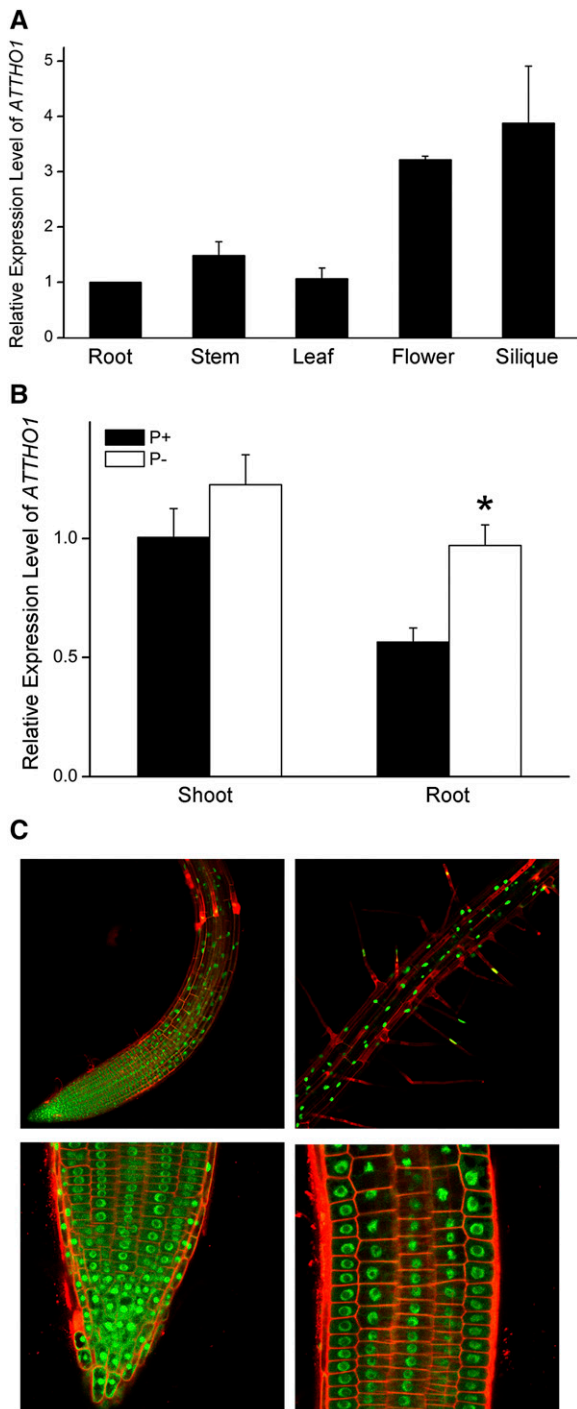
Figure 4. Expression pattern and subcellular localization of AtTHO1. A, Relative expression levels of *AtTHO1* mRNA in roots, stems, leaves, flowers, and siliques. B, Relative expression levels of *AtTHO1* mRNA in shoots and roots of 8-d-old wild-type seedlings grown under P$^+$ and P$^−$ conditions. Asterisks indicate values that are significantly different from that of the wild type under the same growing conditions (Student's *t* test, *P* < 0.05). C, Subcellular localization of GFP-AtTHO1 in roots of transgenic plants. Top, Root meristem and elongation zones (left) and maturation zone (right). Bottom, a magnified view of the meristematic region at the root tip (left) and near the elongation zone (right).

The *hps8* Phenotypes Are Largely Reversed by the Inhibition of Ethylene Signaling

We previously showed that ethylene is a positive regulator of PSI root-associated APase activity (Lei et al., 2011b; Wang et al., 2012; Yu et al., 2012). Because the *hpr1* mutants (*hpr1-4* and *hpr1-5*) exhibit enhanced ethylene signaling (Pan et al., 2012., Xu et al., 2015), we wondered whether the *hps8* mutant phenotypes were caused by enhanced ethylene signaling. Therefore, we first examined the effects of Ag$^+$, an inhibitor of ethylene perception, on the PSI root-associated APase activity and root hair production in *hps8*. The seeds of the wild type and *hps8* were directly sown on P$^+$ and P$^−$ media with or without 10 μM Ag$^+$, and phenotypes were analyzed 8 d after germination. Addition of Ag$^+$ largely blocked the production of root hairs in the wild type under both P$^+$ and P$^−$ conditions and reduced the BCIP staining on the wild-type root surface (Fig. 6A). For *hps8*, addition of Ag$^+$ completely suppressed BCIP staining on the root surface on P$^+$ medium and largely reduced such staining on P$^−$ medium. On P$^−$ medium with Ag$^+$, however, the BCIP staining of *hps8* was still stronger than that of the wild type. We also found that Ag$^+$ could substantially reverse the enhanced production of root hairs by *hps8* under both P$^+$ and P$^−$ conditions, although the inhibition was not as complete as that observed for the wild type (Fig. 6B).

To obtain additional evidence that the enhanced APase activity and root hair production in *hps8* was due to the increased ethylene signaling, we examined the root-associated APase activity and root hair phenotypes in an *hpr1-5* single mutant and in *hpr1-5ein2* and *hpr1-5ein3* double mutants. EIN2 and EIN3 are two positive regulators of ethylene signaling (Zhao and Guo, 2011). *ein2* is completely insensitive to ethylene while *ein3* is only partially insensitive to ethylene. *hpr1-5* exhibited phenotypes similar to those of *hps8* in terms of enhanced root-associated APase activity and root hair production (Fig. 7). In *hpr1-5ein2*, the enhanced root hair production and root-associated APase activity were greatly suppressed under both P$^+$ and P$^−$ conditions. In *hpr1-5ein3*, however, the enhanced root-associated APase activity and root hair production were only slightly suppressed under Pi sufficiency. This was probably because loss of EIN3 function does not completely block ethylene signaling.

Taken together, these results indicated that increased ethylene signaling is largely responsible for the enhanced PSI root-associated APase activity and root hair production in *hps8*.

Regulated miRNA Biogenesis Is Important for the Control of PSI Root-Associated APase Activity

Because the altered ethylene signaling was not completely responsible for enhanced root-associated APase activity in *hps8*, we inferred that other factors must contribute to this mutant phenotype. Previous study showed that mutation in AtTHO1 reduced the accumulation of several miRNAs (Furumizu et al., 2010), suggesting that regulated biogenesis of miRNAs is important for the

Figure 5. Root surface-associated APase activity and root hair patterns in various mutants. A, BCIP staining of APase activities on the root surface of 8-d-old seedlings of the wild type, *hps8*, *attho3*, and *attho6* grown on P$^+$ and P$^-$ media. B, Patterns of root hairs in the seedlings corresponding to those in A.
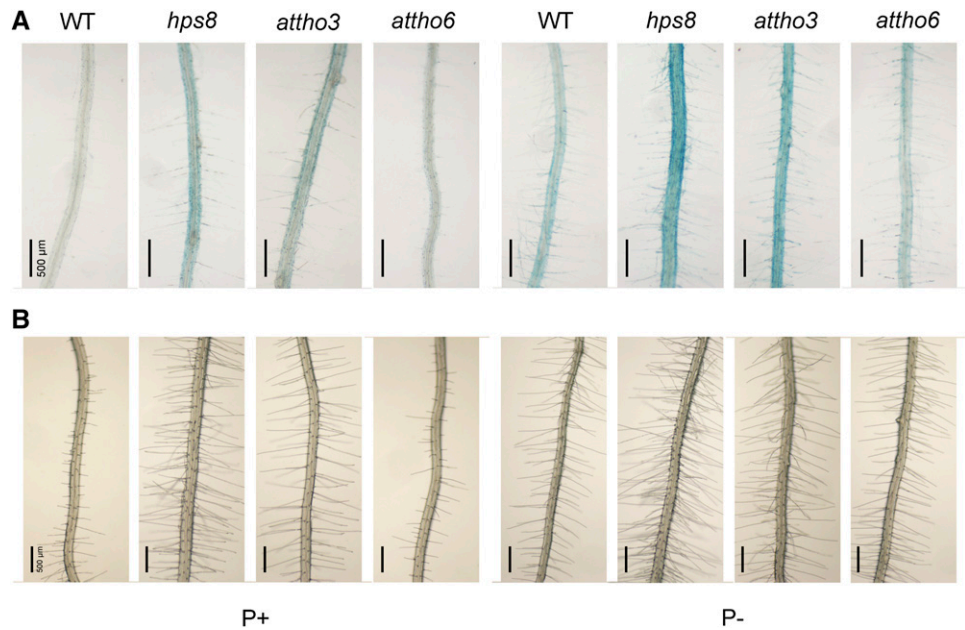
proper control of PSI root-associated APase activity. To test this hypothesis, we first examined root-associated APase activity in five mutants with defects in miRNA biogenesis. In Arabidopsis, the genes *ABH1*, *HASTY*, *SE*, *DCL1*, and *HYL1* are involved in the processing of pri-miRNA to mature miRNA (Yang et al., 2006; Laubinger et al., 2008; Dong et al., 2008). The mutants for these five genes all displayed reduced root-associated APase activity under Pi deficiency as shown by BCIP staining (Supplemental Fig. S5), indicating that regulated miRNA biogenesis is important

for the control of PSI root-associated APase activity (although the phenotypes of these mutants were opposite to those of *hps8*).

The Expression Profiles of miRNAs Are Altered in *hps8*

Next, we investigated how the mutation of *AtTHO1* affects the accumulation of miRNAs at the genomic level. The abundance of mature miRNAs in the wild type and *hps8* was compared using the miRNA-seq

Figure 6. Effects of the ethylene perception inhibitor Ag$^+$ on the root-associated APase activity and root hair production in the wild type and *hps8*. A, BCIP staining of root-associated APase activity of 8-d-old seedlings of the wild type and *hps8* grown on P$^+$ and P$^-$ medium with or without addition of 10 μM Ag$^+$. B, Root hair patterns of the seedlings corresponding to those shown in A.
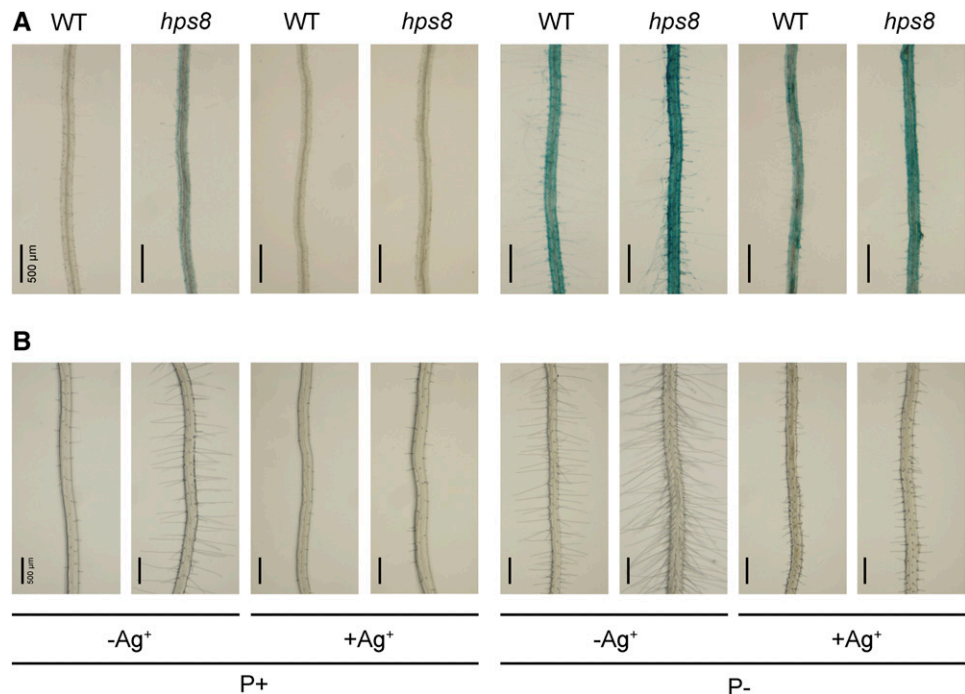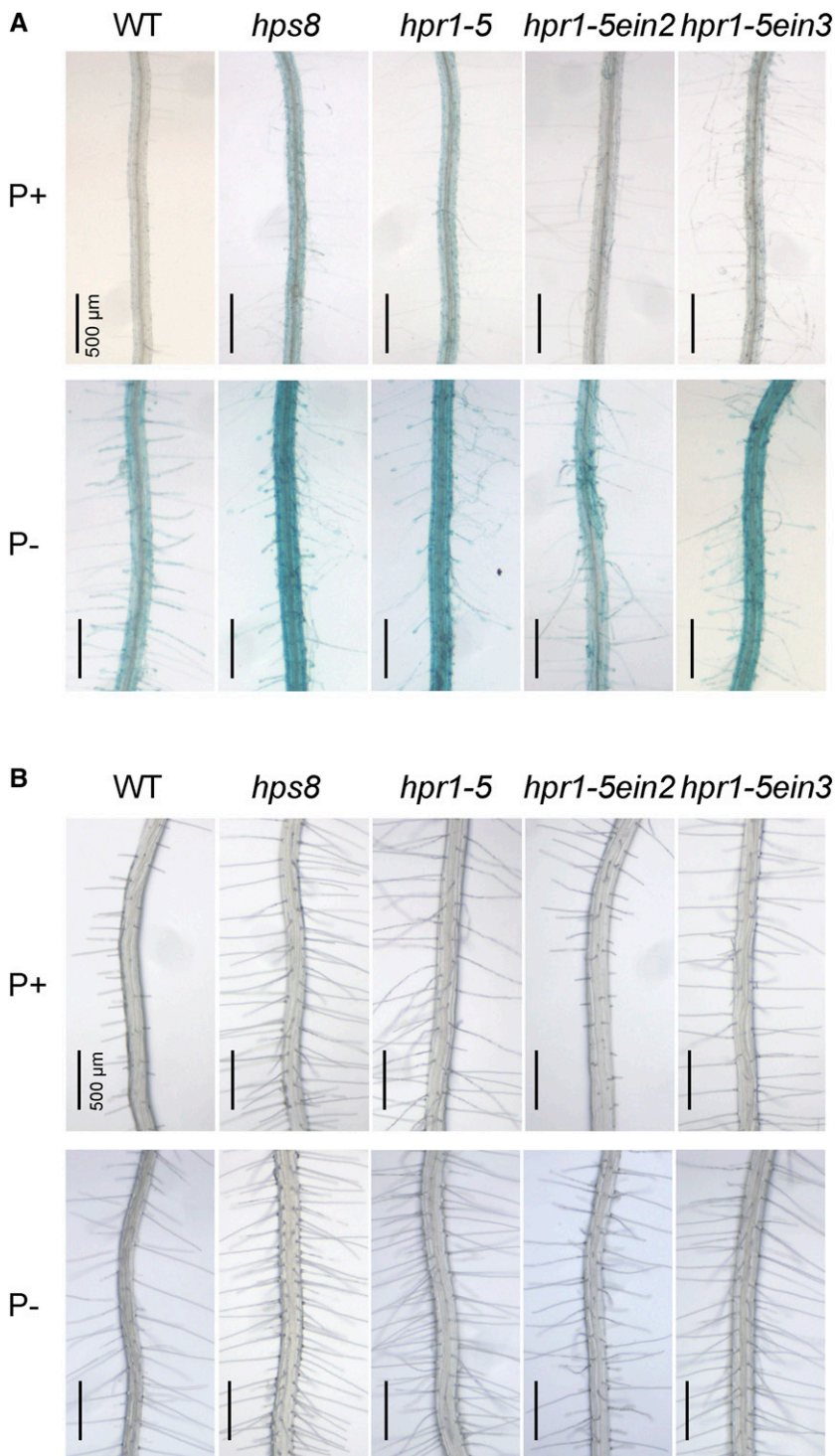
Figure 7. The root-associated APase activity and root hair production of the wild type and various mutants grown under P⁺ and P⁻ conditions. A, Histochemical staining using BCIP as a substrate of APase activity on the root surface of 8-d-old seedlings. B, Root hair patterns of 8-d-old seedlings.

technique. Total RNAs were extracted from the roots of 8-d-old seedlings grown under P⁺ and P⁻ conditions. The RNA samples were fractionated by electrophoresis, and the RNAs with 20 to 50 nucleotides were isolated and subjected to RNA deep sequencing. For four miRNA samples, we generated a total of 83,350,440 short reads (Supplemental Table S2). After the low quality data were filtered, more than four million reads per sample were used to map miRNAs in the Arabidopsis genome (TAIR 9.0). Among the reads for each sample, 79% to 85% could be aligned with the reference genome with perfect match (Supplemental Table S2). Two-hundred-thirty-one annotated miRNAs were detected in the sequenced samples, indicating a robust coverage of miRNAs. We first compared the miRNA expression profiles of the wild type grown under P⁺ and
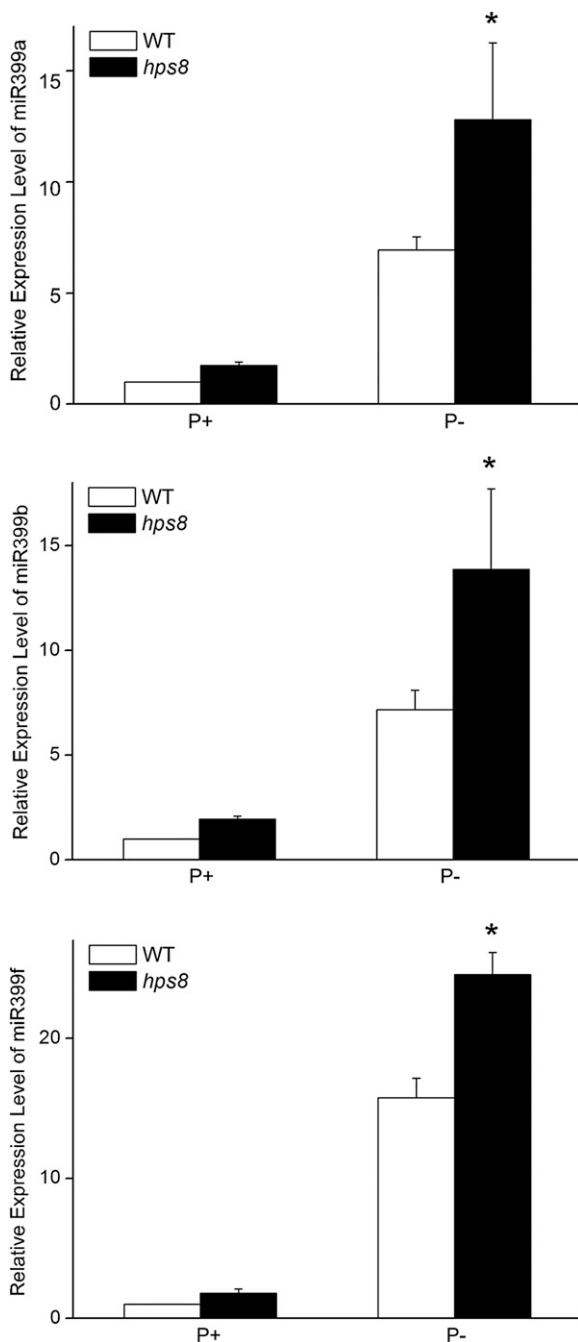
Figure 8. qPCR analysis of relative levels of three mature miRNA399s in the roots of 8-d-old seedlings of the wild type and *hps8* grown under P^+ and P^- conditions. Values are means ± SE with three replicates. Asterisks indicate that the mean is significantly different from that of the wild type (*t*-test, $P < 0.05$).

P^- conditions. The differences in expression level between the two kinds of samples were represented with log2-transformed ratio. After normalization, only the miRNAs with more than 1 read/per million of mapped reads were used for comparison, and the $\log_2$ value of at least 1 was used as the cutoff to select miRNAs that

differentially accumulated in P^+ and P^- wild-type seedlings (*P* value ≤ 0.01). Based on these criteria, 43 miRNAs were up-regulated and 23 miRNAs were down-regulated (Supplemental Table S3) in the roots of Pi-starved wild-type plants. The up-regulation of miRNA156, miRNA157, miRNA167, miRNA172, miRNA399, miRNA827, and miRNA2111, and the down-regulation of miRNA169 and miRNA395 were consistent with previous reports (Pant et al., 2009; Hsieh et al., 2009), indicating that the experimental condition we used for RNA-seq analysis was proper. We then compared the miRNA levels between the wild type and *hps8* under normal growth conditions. Both enhanced and reduced accumulation of miRNAs were observed in *hps8*, indicating that the THO/TREX complex can both positively and negatively regulate the biogenesis of miRNAs. Finally, we examined the levels of the up- and down-regulated miRNAs in *hps8* grown under P- condition. As shown in Supplemental Table S3, the accumulation of miRNA397, miRNA398, miRNA399, and miRNA408 was higher in P- *hps8* than in P^- wild type. Among the down-regulated miRNAs in P^- wild type, the abundance of miRNA169 and miRNA395 was further down-regulated in P^- *hps8*.

Among these differentially expressed miRNAs, miRNA399 plays a critical role in regulating Pi homeostasis in plants (Pant et al., 2008). In our RNA-seq analyses, we also found that the different members of the miRNA399 family were differentially induced by Pi starvation, i.e. miRNA399b, 399c, and 399f were the major contributors to the total amount of induced miRNA399s. Compared to their levels in P^+ wild type, the levels of miRNA399b, 399c, and 399f were enhanced 30-, 31-, and 155- fold, respectively, in P^- wild type. In P^- *hps8*, however, the induction of these three miRNAs was increased by 39-, 38-, and 211-fold, respectively (Supplemental Table S3). The enhanced accumulation of these three mature miRNA399s in *hps8* was confirmed by qPCR (Fig. 8).

The miRNA399-PHO2 Pathway Is Involved in the Regulation of PSI Root-Associated APase Activity

Our comparative miRNA-seq analyses suggested that the alteration of miRNA levels might affect root-associated APase activity. We then examined the root-associated APase activity in a *miRNA399b*-overexpressing line (hereafter referred to as *miRNA399 OX*). There was no blue staining on the root surface of *miRNA399b OX* on P^+ medium (Fig. 9A); under Pi starvation, however, BCIP staining was much stronger on the root surface of *miRNA399 OX* than of the wild type. *PHO2* mRNA encodes a ubiquitin E2 conjugase and is the direct target of miRNA399. Thus, the phenotype of the *pho2* mutant would be expected to be similar to that of *miRNA399 OX*. Indeed, *pho2-1* (hereafter referred to as *pho2*), which contains a point mutation in the sixth exon of the *PHO2* gene (Aung et al., 2006), also showed enhanced BCIP staining on its root
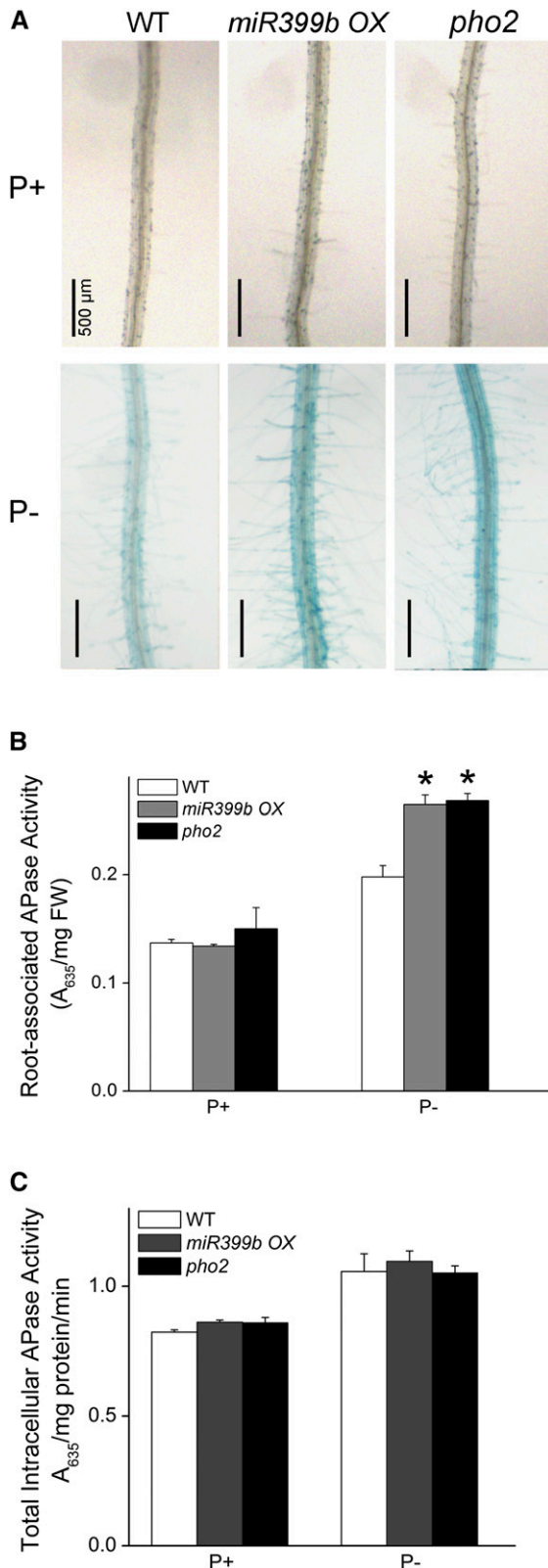
Figure 9. Analysis of Pi starvation-induced root APase activity in 8-d-old Arabidopsis seedlings of the wild type, *miRNA399 OX*, and *pho2* grown under P+ and P− conditions. A, Histochemical staining of APase activity on the root surface of the seedlings using BCIP as a substrate. B,

surface under Pi deficiency (Fig. 9A). The enhanced root-associated APase activity in *miRNA399 OX* and *pho2* was confirmed by quantitative analysis of APase activity using BCIP as the substrate (Fig. 9B). To determine the cause of the enhanced root-associated APase activity in *miRNA399 OX* and *pho2*, we analyzed the transcription of three major APase genes: *AtPAP10*, *AtPAP12*, and *AtPAP26*. The results showed that the transcription of these three APase genes did not differ from that of the wild type under Pi sufficiency (Supplemental Fig. S6); under Pi deficiency, however, the transcription of *AtPAP10* and *AtPAP12* was slightly but significantly increased in *miRNA399 OX* and *pho2* while that of *AtPAP26* remained unchanged. As was the case with *hps8*, total root intracellular APase activity of *miRNA399 OX* and *pho2* did not significantly differ from that of the wild type under both P+ and P− conditions (Fig. 9C). These results suggested that the miRNA399-PHO2 pathway positively regulates the secretion of APase proteins or their enzymatic activities on the root surface. Unlike *hps8* and other ethylene-related mutants, *miRNA399 OX* and *pho2* did not overproduce root hairs under normal growth conditions (Supplemental Fig. S7).

DISCUSSION

Induction and secretion of APases is an important strategy that plants use to cope with Pi deficiency in their environment. The regulatory mechanism underlying this adaptive response, however, has been largely unknown. To identify the molecular components involved in the regulation of PSI root-associated APase activity, we performed a genetic screen for Arabidopsis mutants with altered root-associated APase activity. From this screen, we obtained a series of *hps* (*hypersensitive to Pi starvation*) mutants with enhanced root-associated APase activity. *hps2* is a new allele of *CTR1*, which is a key regulator of ethylene signaling (Lei et al., 2011a, 2011b). Knockout of the *CTR1* gene causes plants to display constitutive ethylene responses (Kieber et al., 1993). *HPS3* encodes ETHYLENE OVERPRODUCTION1 (Wang et al., 2004, 2012), which, when mutated, results in the overproduction of ethylene in Arabidopsis seedlings. *hps4* contains a mutation in the *SABRE* gene. The SABRE protein was found to antagonistically interact with ethylene signaling to regulate Pi responses (Yu et al., 2012). We also obtained mutants with enhanced root-associated APase activity that did not result from altered ethylene biosynthesis or signaling. These mutants included *hps7*, *hps9*, and *hps10*. HPS7 is a tyrosylprotein sulfotransferase that suppresses the expression of many photosynthetic genes in roots (Kang et al., 2014). For *hps9* and *hps10*, the mutated genes

Root surface-associated APase activity as determined with BCIP as the substrate. C, Root intracellular APase activity as determined with BCIP as the substrate. Values in B and C represent means with SE of three replicates. Asterisks indicate a significant difference (*P* < 0.05) from the wild type according to Student's *t*-test.

responsible for enhanced root-associated APase activity encode proteins localized in the Golgi apparatus and tonoplasts, respectively (unpublished data). These results indicated that the induction of root-associated APase activity by Pi starvation is regulated by multiple pathways.

In this work, we identified an Arabidopsis mutant, *hps8*, based on the alteration of root-associated APase activity. *hps8* has enhanced root-associated APase activity under both Pi sufficiency and deficiency (Fig. 1). Although the transcription of two major APase genes, *AtPAP10* and *AtPAP12*, was slightly changed, the total intracellular APase activity in *hps8* is similar to that of the wild type. This suggested that the enhanced PSI root-associated APase activity in *hps8* is due to the increased secretion of APase proteins or to the increased enzymatic activity of APases on the root surface. Compared to the wild type, this mutant also produces more root hairs and has smaller plant stature (Figs. 2 and 3). Our molecular and genetic analyses demonstrated that these mutant phenotypes result from a point mutation in the *AtTHO1* gene (Fig. 3). AtTHO1 shares homology with HPR1, a subunit of the THO/TREX protein complex that is highly conserved in yeast, animals, and humans (Strässer et al., 2002; Rehwinkel et al., 2004; Katahira, 2012). In these organisms, the THO/TREX complex functions in transcription elongation and mRNA export from the nucleus. Previous research provided evidence that this complex also exists in Arabidopsis. First, the genes encoding all seven subunits of the THO/TREX complex have been identified in the Arabidopsis genome (Yelina et al., 2010). Second, the proteins corresponding to the six subunits of this complex have been found in the nuclei of Arabidopsis cells (Yelina et al., 2010). Our results also confirmed that AtTHO1 is a nucleus-localized protein (Fig. 4). Third, mutation in two subunits of this complex, AtTHO1 and AtTHO3, results in similar developmental defects and impaired biogenesis of tasiRNAs (Yelina et al., 2010; Jauvion et al., 2010). We also found that the mutants *attho1* and *attho3* both overproduce roots hairs and have enhanced root-associated APase activity under P$^+$ and P$^-$ conditions (Fig. 5), further indicating that AtTHO1 and AtTHO3 exist as subunits of the same protein complex in Arabidopsis. In addition to functioning in mRNA export in Arabidopsis (Pan et al., 2012; Xu et al., 2015), this THO/TREX complex is involved in the biogenesis of miRNA (Yelina et al., 2010; Jauvion et al., 2010; Furumizu et al., 2010). As observed in the other mutant alleles of the *AtTHO1* gene, the abundance of several miRNAs is altered in *hps8* (Supplemental Table S3). Interestingly, the defects in the THO/TREX complex can either enhance or reduce the accumulation of mature miRNAs. This indicates that the roles of the THO/TREX complex in regulating miRNA biogenesis could differ depending on the species of miRNA.

As noted earlier, we previously demonstrated that ethylene is a positive regulator of root-associated APase activity induced by Pi starvation by analyzing the three *hps* mutants: *hps2*, *hps3*, and *hps4* (Lei et al., 2011a, 2011b; Wang et al., 2012; Yu et al., 2012). All of these mutants show enhanced root-associated APase activity under Pi starvation. They also exhibit light-blue BCIP staining on their root surfaces, and they overproduce root hairs under normal growth conditions. Moreover, the total root intracellular APase activities of these three mutants do not significantly differ from that of the wild type under Pi deficiency, indicating that ethylene mainly affects the secretion of APases or the enzymatic activity of APases on the root surface. The APase phenotype of *hps8* is very similar to the APase phenotypes of these three *hps* mutants, suggesting that the enhanced root-associated APase activity in *hps8* might also result from enhanced ethylene signaling due to a mutation in the *AtTHO1* gene. Consistent with this inference, *hpr1-4* (a mutant allele of *AtTHO1*) has enhanced sensitivity to ethylene-induced senescence (Pan et al., 2012). Recently, Xu et al. (2015) reported that *hpr1-5*, another mutant allele of *AtTHO1*, has enhanced ethylene signaling. They further showed that AtTHO1 regulates the expression of *REVERSION-TO-ETHYLENE1*, which represses ethylene responses by promoting the activity of the ethylene receptor ETR1. When AtTHO1 is mutated, it reduces the expression of *REVERSION-TO-ETHYLENE1*, which derepresses ethylene responses by suppressing the activity of ETR1. Our experiments using the ethylene-perception inhibitor Ag$^+$ suggest that the enhanced root-associated APase activity in *hps8* is mainly caused by increased ethylene signaling (Fig. 6). Furthermore, we found that the enhanced root-associated APase activity in *hpr1-5* is reversed in the *hpr1-5ein2* and *hpr1-5ein3* double mutants (Fig. 7). *ein2* and *ein3* are two ethylene-insensitive mutants that have defects in ethylene signaling (Zhao and Guo et al., 2011). *ein2* is completely insensitive to ethylene whereas *ein3* is only partially insensitive to ethylene. The levels of suppression of enhanced root-associated APase activity and root hair production in these two double mutants are correlated with the degree of their insensitivity to ethylene (*hpr1-5ein2* > *hpr1-5ein3*). This experiment provided additional evidence that the enhanced root-associated APase activity in *hps8* results from the increased ethylene signaling. Although increased root hair production may also contribute to the total root-associated APase activity in *hps8*, the enhanced BCIP staining in nonroot hair cells further indicated that the enhanced root-associated APase activity in *hps8* was mainly due to the direct regulation by ethylene signaling. Based on these results, we conclude that the THO/TREX complex negatively regulates PSI root-associated APase activity by suppressing ethylene signaling.

Enhanced ethylene biosynthesis or signaling has previously been shown to inhibit primary root growth (Růzicka et al., 2007). Interestingly, this inhibition is not evident in *hps8*. We speculate that the enhancement of ethylene signaling in *hps8* is too weak to inhibit primary root growth but is strong enough to enhance root hair production. In other words, production of root hairs might be more sensitive than primary root growth to ethylene.

Although enhanced ethylene signaling is largely responsible for the *hps8* mutant phenotypes, the application of Ag$^+$ did not completely reverse enhanced

root-associated APase activity in *hps8*. Similarly, in *hpr5-1ein2*, the enhanced root-associated APase activity is not completely suppressed. These results suggest that other factors must also contribute to *hps8* mutant phenotypes. Because the THO/TREX complex is involved in the biogenesis of miRNAs, we wondered whether miRNA homeostasis is important in regulating PSI root-associated APase activity. Indeed, we found that the five Arabidopsis mutants with defects in miRNA biogenesis had reduced root-associated APase activity (Supplemental Fig. S5). We then investigated whether the altered expression of miRNAs could affect the root-associated APase activity. Our miRNA-seq analyses revealed that the levels of 22 miRNA species, including several members of miRNA399 family, were elevated in *hps8* under both P$^+$ and P$^-$ conditions (Supplemental Table S3). miRNA399 has been shown to play a critical role in the maintenance of Pi homeostasis in plants (Liu et al., 2012; Huang et al., 2013). This prompted us to examine the phenotypes of the *miRNA399 OX* and the mutant of the *PHO2* gene whose mRNA is the direct target of miRNA399. Our results showed that the *miRNA399 OX* and *pho2* mutants both display enhanced root-associated APase phenotypes under Pi starvation. These results also demonstrate that the enhancement of root-associated APase activity caused by overexpression of miRNA399 is likely to be mediated by the degradation of *PHO2* mRNA. Zhang et al. (2011) also reported that root-associated APase activity is enhanced in the *pho2* mutant of rice, providing another line of evidence for the involvement of the miRNA399-PHO2 pathway in the control of PSI root-associated APase activity. However, *miRNA399 OX* and *pho2* did not show light-blue BCIP staining under normal growth conditions (Fig. 9). In addition, ethylene does not affect the transcription of *AtPAP10* under P$^-$ condition (Zhang et al., 2014), but the transcription of *AtPAP10* is increased in *miRNA399 OX* and *pho2* (Supplemental Fig. S6). These results suggest that the molecular mechanism by which the miRNA399-PHO2 pathway regulates the induction of root-associated APase activity by Pi starvation may be independent of ethylene production.

Finally, although the analysis of *hps8* led us to discover the role of miRNA399-PHO2 pathway in the regulation of PSI root-associated APase activity, the results do not seem to indicate a direct link between the increased expression of miRNA399 and enhanced root-associated APase activity in *hps8*. These results include: (1) Pi overaccumulates in *miRNA399 OX* and *pho2* shoots but not in *hps8* shoots (Supplemental Fig. S3); and (2) In *hps8*, the level of *PHO2* mRNA, which is the direct target of miRNA399, is not significantly reduced compared to that of the wild type (data not shown). Of course, we cannot exclude the possibility that a mild increase in the expression of miRNA399 is insufficient to perturb the Pi homeostasis in shoots but is sufficient to enhance PSI root-associated APase activity. Therefore, further investigation is needed to find components in addition to enhanced ethylene signaling

that contribute to the increased root-associated APase activity in *hps8*.

In summary, we identified an Arabidopsis mutant, *hps8*, with enhanced PSI root-associated APase activity. The *hps8* mutant carries a mutation in the THO/TREX complex, a complex that is involved in mRNA export and miRNA biogenesis in Arabidopsis. Subsequent analyses of *hps8* indicated that the THO/TREX complex negatively regulates root-associated APase activity by suppressing ethylene signaling. In *hps8*, the expression of several miRNAs is altered, including the enhanced expression of miRNA399. The characterization of *hps8* also led us to discover that the miRNA399-PHO2 signaling pathway is involved in the regulation of PSI root-associated APase activity. The next challenge will be to elucidate how the ethylene signaling and miRNA399-PHO2 pathways regulate this important adaptive response of plants to Pi starvation.

MATERIALS AND METHODS

Plant Growth Conditions

Arabidopsis (*Arabidopsis thaliana*) plants of the Columbia ecotype were used as the wild type in this study. Half-strength MS medium with 1% (w/v) Suc and 1.2% (w/v) agar (Cat. no. A1296; Sigma-Aldrich) was used as the Pi-sufficient (P$^+$) medium. The Pi-deficient medium (P$^-$) was made by replacing the 0.625 mM KH$_2$PO$_4$ with 0.625 mM K$_2$SO$_4$ in the P$^+$ medium. Seeds were surface-sterilized with 20% (v/v) bleach for 15 min. After four washes in sterile-distilled water, seeds were sown on petri plates containing P$^+$ or P$^-$ medium. After the seeds were stratified at 4°C for 2 d, the agar plates were placed vertically in a growth room at 22 to 24°C and with a photoperiod of 16 h of light and 8 h of darkness. The light intensity was 100 μmol m^{-2} s^{-1}.

Mutant Isolation

Approximately 100,000 EMS-mutagenized M$_2$ seeds representing 6000 M$_1$ plant lines were used for mutant screening. After the seedlings had grown on P$^-$ medium for 8 d, the roots were overlaid with a 0.5% agar solution containing 0.01% BCIP for 24 h at 23°C (Wang et al., 2011).The seedlings with enhanced BCIP staining relative to the wild type were identified as putative mutants and were transferred to soil. The plants were self-pollinated to produce progeny, and the mutant phenotypes were retested in the next generation. The mutants were back-crossed to the wild-type plants two times before they were further characterized.

Analysis of Root APase Activity

Histochemical and quantitative analyses of root intracellular and root-associated APase activities were performed as described by Wang et al. (2011).

Molecular Cloning of the *HPS8* Gene

The mutant *hps8* was crossed to a plant of the Landsberg *erecta* ecotype to generate a mapping population. The F2 progeny that displayed dark-blue BCIP staining on their root surfaces were selected, and DNAs from these seedlings were extracted for molecular mapping. A set of SSLP and CAPS markers was used to map the *HPS8* gene. The sequences and chromosomal positions of the molecular markers are listed in Supplemental Table S1.

Vector Construction and Plant Transformation

For genetic complementation of the *hps8* mutant, the wild-type genomic sequence of the *AtTHO1* gene was amplified from the Arabidopsis genomic DNA using the primers 5'-GTCGACCCACTCTTCTTCAAGTTTGGG-3' and 5'-ACTAGTACAAACTGAAAGCGTATTCA-3'. During amplification, the

restriction enzyme sites of *Sal*I and *Spe*I were added to the 5′ and 3′ ends, respectively, of the PCR product. The PCR product was ligated to the pEASY vector and verified for accuracy by sequencing. The *AtTHO1* gene was then excised from the pEASY vector with *Sal*I and *Spe*I enzymes and was used to replace the luciferase gene located between the 35S CaMV promoter and NOS terminator on the plant transformation vector pZhou. The resulting construct was named *35S CaMV:AtTHO1*.

For subcellular localization of AtTHO1 protein, the protein coding sequence (CDS) of the *AtTHO1* gene was PCR-amplified from Arabidopsis cDNAs using the primers 5′-CCCGGGATGGATGCATTTAGAGATGCTA-3′ and 5′-AAGCTTT-CATGAGACGGGCATAGGA-3′. The *Xba*I and *Hind*III restriction enzyme sites were added to the 5′ and 3′ ends of the amplified CDS of the AtTHO1 gene. The amplified CDS was digested with *Xba*I and *Hind*III enzymes and cloned into the pEGAD vector to create the construct *35S CaMV:GFP-AtTHO1*.

Both plant transformation vectors were mobilized into *Agrobacterium tumefaciens* strain GV3101 and transformed into Arabidopsis plants using the floral dip method (Clough and Bent, 1998).

Quantitative Real-Time PCR

Total RNAs were extracted from 8-d-old seedlings, and quantitative real-time PCR was performed as described by Wang et al. (2011). The primers used for detection of the mRNA expression for *HPS8* are as follows: 5′-TCCAGTGCCT-CATTATGTTTGA-3′ (forward) and 5′-TGACTTAAGTTCTTCCTTCATGGTT-3 (reverse). The *ACTIN* gene was used as an internal control.

miRNA-Seq Analysis

Total RNAs were isolated from the roots of 8-d-old seedlings using the RNeasy Plant Mini Kit (Qiagen). The RNA samples were fractionated by electrophoresis, and the RNAs with 20 to 50 nucleotides were isolated and subjected to miRNA deep sequencing using a HiSEquation 2000 system (Illumina) with standard settings. The raw data of Illumina reads has been deposited into the NCBI Sequence Read Archive under accession no. SRP073352. The raw data were filtered to remove reads shorter than 18 nucleotides or longer than 28 nucleotides, as well as reads with poor quality. The remaining reads were mapped to the Arabidopsis reference genome (TAIR9) with exact match using bowtie. The expression counts of each miRNA were calculated and were normalized to reads per million (RPMs) mapped reads. Only the miRNAs with the expression level higher than 1.0 RPM were used for further analyses. The cutoff value for differential expression was a >2-fold change in expression with a P value ≤ 0.01.

qPCR Analysis for the Abundance of Mature miRNAs

Total RNAs were extracted with TRIzol reagent (Invitrogen) from 8-d-old seedlings grown on P^+ and P^- media. After the extracted RNAs were treated with RNase-free DNase I (Promega) to remove DNA contamination, 150 ng of total RNA was polyadenylated and reverse-transcribed using the Mir-X miRNA First Strand Synthesis Kit (Cat. no. 638315; Takara). miRNAs were detected using the Mir-X miRNA qRT-PCR SYBR Kit (Cat. no. 638314; Takara). Primers used for PCR analyses of each miRNA are listed in Supplemental Table S4.

Microscopy

The root hairs of the 8-d-old seedlings were examined with a stereomicroscope (model no. SZ61; Olympus).

For subcellular localization of the AtTHO1 protein, 8-d-old *35S::GFP-AtTHO1* seedlings were used for confocal microscopic analysis. The roots were excised from the seedlings and stained with 10 μM propidium iodide (PI) for 5 s and rinsed with distilled water. The specimens were examined with a confocal laser scanning microscope (710META; Zeiss). Excitation wavelengths of 546 and 488 nm were used to visualize the signals of PI staining and GFP, respectively. The emission wavelengths for PI and GFP were 573 and 507 nm.

Accession Numbers

Sequence data from this article can be found in The Arabidopsis Information Resource database under the following accession numbers: AtTHO1 (At5g09860), AtTHO2 (At1g24706), AtTHO3 (At5g56130), AtTHO6 (At2g19430), EIN2 (At5g03280), and EIN3 (At3g20770).

Supplemental Data

The following supplemental materials are available.

Supplemental Figure S1. Relative expression of three major APase genes in the roots of wild-type and *hps8* seedlings.

Supplemental Figure S2. The root cell length and root meristem size of wild-type and *hps8* seedlings grown under normal growth conditions.

Supplemental Figure S3. The contents of total P and cellular Pi in shoots and roots of the wild type and *hps8*.

Supplemental Figure S4. The mapping strategy for the *HPS8* gene. The molecular markers used in the fine mapping are shown above the horizontal lines. The numbers below each horizontal line are the AGI coordinates on the chromosome. Distance unit: Mb.

Supplemental Figure S5. PSI root-associated APase activity of the wild type and five mutants that are defective in miRNA biogenesis.

Supplemental Figure S6. Relative expression of three major APase genes in roots of seedlings of the wild type, *miRNA399 OX*, and *pho2*.

Supplemental Figure S7. Patterns of root hairs of the wild type, *miRNA399 OX*, and *pho2*.

Supplemental Table S1. Molecular markers used for map-based cloning of the *HPS8* gene.

Supplemental Table S2. Summary of the miRNA reads generated from miRNA-seq analysis.

Supplemental Table S3. Up- and down-regulated miRNAs in Pi-starved wild-type plants and their expression in *hps8*.

Supplemental Table S4. Sequences for the primers for qPCR analysis of mature miR399s.

LITERATURE CITED

Aung K, Lin SI, Wu CC, Huang YT, Su CL, Chiou TJ (2006) *pho2*, a phosphate overaccumulator, is caused by a nonsense mutation in a microRNA399 target gene. Plant Physiol **141:** 1000–1011

Clough SJ, Bent AF (1998) Floral dip: a simplified method for *Agrobacterium*-mediated transformation of Arabidopsis thaliana. Plant J **16:** 735–743

del Pozo JC, Allona I, Rubio V, Leyva A, de la Peña A, Aragoncillo C, Paz-Ares J (1999) A type 5 acid phosphatase gene from *Arabidopsis thaliana* is induced by phosphate starvation and by some other types of phosphate mobilising/oxidative stress conditions. Plant J **19:** 579–589

Del Vecchio HA, Ying S, Park J, Knowles VL, Kanno S, Tanoi K, She YM, Plaxton WC (2014) The cell wall-targeted purple acid phosphatase At-PAP25 is critical for acclimation of *Arabidopsis thaliana* to nutritional phosphorus deprivation. Plant J **80:** 569–581

Dong Z, Han MH, Fedoroff N (2008) The RNA-binding proteins HYL1 and SE promote accurate in vitro processing of pri-miRNA by DCL1. Proc Natl Acad Sci USA **105:** 9970–9975

Furumizu C, Tsukaya H, Komeda Y (2010) Characterization of EMU, the Arabidopsis homolog of the yeast THO complex member HPR1. RNA **16:** 1809–1817

Goldstein AH, Baertlein DA, McDaniel RG (1988) Phosphate starvation inducible metabolism in *Lycopersicon esculentum*: 1. Excretion of acid-phosphatase by tomato plants and suspension-cultured cells. Plant Physiol **87:** 711–715

Hsieh LC, Lin SI, Shih AC, Chen JW, Lin WY, Tseng CY, Li WH, Chiou TJ (2009) Uncovering small RNA-mediated responses to phosphate deficiency in Arabidopsis by deep sequencing. Plant Physiol **151:** 2120–2132

Huang TK, Han CL, Lin SI, Chen YJ, Tsai YC, Chen YR, Chen JW, Lin WY, Chen PM, Liu TY, et al (2013) Identification of downstream

components of ubiquitin-conjugating enzyme PHOSPHATE2 by quantitative membrane proteomics in Arabidopsis roots. Plant Cell 25: 4044–4060

Hurley BA, Tran HT, Marty NJ, Park J, Snedden WA, Mullen RT, Plaxton WC (2010) The dual-targeted purple acid phosphatase isozyme At-PAP26 is essential for efficient acclimation of Arabidopsis to nutritional phosphate deprivation. Plant Physiol 153: 1112–1122

Jauvion V, Elmayan T, Vaucheret H (2010) The conserved RNA trafficking proteins HPR1 and TEX1 are involved in the production of endogenous and exogenous small interfering RNA in Arabidopsis. Plant Cell 22: 2697–2709

Kang J, Yu H, Tian C, Zhou W, Li C, Jiao Y, Liu D (2014) Suppression of photosynthetic gene expression in roots is required for sustained root growth under phosphate deficiency. Plant Physiol 165: 1156–1170

Kant S, Peng M, Rothstein SJ (2011) Genetic regulation by NLA and microRNA827 for maintaining nitrate-dependent phosphate homeostasis in Arabidopsis. PLoS Genet 7: e1002021

Katahira J (2012) mRNA export and the TREX complex. Biochim Biophys Acta 1819: 507–513

Kieber JJ, Rothenberg M, Roman G, Feldmann KA, Ecker JR (1993) CTR1, a negative regulator of the ethylene response pathway in Arabidopsis, encodes a member of the raf family of protein kinases. Cell 72: 427–441

Kuo HF, Chiou TJ (2011) The role of microRNAs in phosphorus deficiency signaling. Plant Physiol 156: 1016–1024

Laubinger S, Sachsenberg T, Zeller G, Busch W, Lohmann JU, Rätsch G, Weigel D (2008) Dual roles of the nuclear cap-binding complex and SERRATE in pre-mRNA splicing and microRNA processing in Arabidopsis thaliana. Proc Natl Acad Sci USA 105: 8795–8800

Lei M, Liu Y, Zhang B, Zhao Y, Wang X, Zhou Y, Raghothama KG, Liu D (2011a) Genetic and genomic evidence that sucrose is a global regulator of plant responses to phosphate starvation in Arabidopsis. Plant Physiol 156: 1116–1130

Lei M, Zhu C, Liu Y, Karthikeyan AS, Bressan RA, Raghothama KG, Liu D (2011b) Ethylene signalling is involved in regulation of phosphate starvation-induced gene expression and production of acid phosphatases and anthocyanin in Arabidopsis. New Phytol 189: 1084–1095

Lenburg ME, O'Shea EK (1996) Signaling phosphate starvation. Trends Biochem Sci 21: 383–387

Li D, Zhu H, Liu K, Liu X, Leggewie G, Udvardi M, Wang D (2002) Purple acid phosphatases of Arabidopsis thaliana. Comparative analysis and differential regulation by phosphate deprivation. J Biol Chem 277: 27772–27781

Liang G, Yang F, Yu D (2010) MicroRNA395 mediates regulation of sulfate accumulation and allocation in Arabidopsis thaliana. Plant J 62: 1046–1057

Lin WY, Huang TK, Chiou TJ (2013) Nitrogen limitation adaptation, a target of microRNA827, mediates degradation of plasma membrane-localized phosphate transporters to maintain phosphate homeostasis in Arabidopsis. Plant Cell 25: 4061–4074

Linkohr BI, Williamson LC, Fitter AH, Leyser HM (2002) Nitrate and phosphate availability and distribution have different effects on root system architecture of Arabidopsis. Plant J 29: 751–760

Liu TY, Huang TK, Tseng CY, Lai YS, Lin SI, Lin WY, Chen JW, Chiou TJ (2012) PHO2-dependent degradation of PHO1 modulates phosphate homeostasis in Arabidopsis. Plant Cell 24: 2168–2183

Mallory AC, Vaucheret H (2006) Functions of microRNAs and related small RNAs in plants. Nat Genet (Suppl) 38: S31–S36

Margis R, Fusaro AF, Smith NA, Curtin SJ, Watson JM, Finnegan EJ, Waterhouse PM (2006) The evolution and diversification of Dicers in plants. FEBS Lett 580: 2442–2450

Pan H, Liu S, Tang D (2012) HPR1, a component of the THO/TREX complex, plays an important role in disease resistance and senescence in Arabidopsis. Plant J 69: 831–843

Pant BD, Buhtz A, Kehr J, Scheible WR (2008) MicroRNA399 is a long-distance signal for the regulation of plant phosphate homeostasis. Plant J 53: 731–738

Pant BD, Musialak-Lange M, Nuc P, May P, Buhtz A, Kehr J, Walther D, Scheible WR (2009) Identification of nutrient-responsive Arabidopsis and rapeseed microRNAs by comprehensive real-time polymerase chain reaction profiling and small RNA sequencing. Plant Physiol 150: 1541–1555

Raghothama KG (2000) Phosphate transport and signaling. Curr Opin Plant Biol 3: 182–187

Rehwinkel J, Herold A, Gari K, Köcher T, Rode M, Ciccarelli FL, Wilm M, Izaurralde E (2004) Genome-wide analysis of mRNAs regulated by the THO complex in Drosophila melanogaster. Nat Struct Mol Biol 11: 558–566

Robinson WD, Park J, Tran HT, Del Vecchio HA, Ying S, Zins JL, Patel K, McKnight TD, Plaxton WC (2012) The secreted purple acid phosphatase isozymes AtPAP12 and AtPAP26 play a pivotal role in extracellular phosphate-scavenging by Arabidopsis thaliana. J Exp Bot 63: 6531–6542

Růzicka K, Ljung K, Vanneste S, Podhorská R, Beeckman T, Friml J, Benková E (2007) Ethylene regulates root growth through effects on auxin biosynthesis and transport-dependent auxin distribution. Plant Cell 19: 2197–2212

Strässer K, Masuda S, Mason P, Pfannstiel J, Oppizzi M, Rodriguez-Navarro S, Rondón AG, Aguilera A, Struhl K, Reed R, Hurt E (2002) TREX is a conserved complex coupling transcription with messenger RNA export. Nature 417: 304–308

Tran HT, Hurley BA, Plaxton WC (2010a) Feeding hungry plants: the role of purple acid phosphatases in phosphate nutrition. Plant Sci 179: 14–27

Tran HT, Qian W, Hurley BA, She YM, Wang D, Plaxton WC (2010b) Biochemical and molecular characterization of AtPAP12 and AtPAP26: the predominant purple acid phosphatase isozymes secreted by phosphate-starved Arabidopsis thaliana. Plant Cell Environ 33: 1789–1803

Veljanovski V, Vanderbeld B, Knowles VL, Snedden WA, Plaxton WC (2006) Biochemical and molecular characterization of AtPAP26, a vacuolar purple acid phosphatase up-regulated in phosphate-deprived Arabidopsis suspension cells and seedlings. Plant Physiol 142: 1282–1293

Wang KL, Yoshida H, Lurin C, Ecker JR (2004) Regulation of ethylene gas biosynthesis by the Arabidopsis ETO1 protein. Nature 428: 945–950

Wang L, Dong J, Gao Z, Liu D (2012) The Arabidopsis gene hypersensitive to phosphate starvation3 encodes ethylene overproduction 1. Plant Cell Physiol 53: 1093–1105

Wang L, Li Z, Qian W, Guo W, Gao X, Huang L, Wang H, Zhu H, Wu JW, Wang D, Liu D (2011) The Arabidopsis purple acid phosphatase At-PAP10 is predominantly associated with the root surface and plays an important role in plant tolerance to phosphate limitation. Plant Physiol 157: 1283–1299

Wang L, Lu S, Zhang Y, Li Z, Du X, Liu D (2014) Comparative genetic analysis of Arabidopsis purple acid phosphatases AtPAP10, AtPAP12, and AtPAP26 provides new insights into their roles in plant adaptation to phosphate deprivation. J Integr Plant Biol 56: 299–314

Wang X, Wang Y, Tian J, Lim BL, Yan X, Liao H (2009) Overexpressing At-PAP15 enhances phosphorus efficiency in soybean. Plant Physiol 151: 233–240

Wanner BL (1996) Phosphorus assimilation and control of the phosphate regulon. In FC Neidhardt , R Curtiss III, JL Ingraham, ECC Lin, KB Low, B Magasanik, WS Reznikoff, M Riley, M Schaechter, HE Umbrager, eds, Escherichia coli and Salmonella: Cellular and Molecular Biology, American Society for Microbiology, Washington, DC, pp 1357–1381

Williamson LC, Ribrioux SP, Fitter AH, Leyser HM (2001) Phosphate availability regulates root system architecture in Arabidopsis. Plant Physiol 126: 875–882

Xu C, Zhou X, Wen CK (2015) HYPER RECOMBINATION1 of the THO/TREX complex plays a role in controlling transcription of the REVERSION-TO-ETHYLENE SENSITIVITY1 gene in Arabidopsis. PLoS Genet 11: e1004956

Yang L, Liu Z, Lu F, Dong A, Huang H (2006) SERRATE is a novel nuclear regulator in primary microRNA processing in Arabidopsis. Plant J 47: 841–850

Yelina NE, Smith LM, Jones AME, Patel K, Kelly KA, Baulcombe DC (2010) Putative Arabidopsis THO/TREX mRNA export complex is involved in transgene and endogenous siRNA biosynthesis. Proc Natl Acad Sci USA 107: 13948–13953

Yu H, Luo N, Sun L, Liu D (2012) HPS4/SABRE regulates plant responses to phosphate starvation through antagonistic interaction with ethylene signalling. J Exp Bot 63: 4527–4538

Yuan H, Liu D (2008) Signaling components involved in plant responses to phosphate starvation. J Integr Plant Biol 50: 849–859

Zhang Q, Wang C, Tian J, Li K, Shou H (2011) Identification of rice purple acid phosphatases related to phosphate starvation signalling. Plant Biol (Stuttg) 13: 7–15

Zhang Y, Wang X, Lu S, Liu D (2014) A major root-associated acid phosphatase in Arabidopsis, AtPAP10, is regulated by both local and systemic signals under phosphate starvation. J Exp Bot 65: 6577–6588

Zhao Q, Guo HW (2011) Paradigms and paradox in the ethylene signaling pathway and interaction network. Mol Plant 4: 626–634

Zhu H, Qian W, Lu X, Li D, Liu X, Liu K, Wang D (2005) Expression patterns of purple acid phosphatase genes in Arabidopsis organs and functional analysis of AtPAP23 predominantly transcribed in flower. Plant Mol Biol 59: 581–594